A Novel Detection Method for Interface Defect Development of High-Speed Train Cable Terminal

Yujing Tang, Yuqi Xu, Guoqiang Gao, Kai Liu, Kui Chen, and Guangning Wu

Abstract As the weak link of the cable assembly, the internal insulation structure of the cable terminal is complex, the installation requirements are high, and the operating environment is complex, which is prone to external interference and insulation failure. However, the existing detection means of the cable terminal of the rolling stock is complicated, expensive, vulnerable to field noise interference and inefficient detection. In this study, a new method for diagnosis of cable termination insulation status by measuring the field strength along the cable termination surface is proposed. The characteristics of axial electric field distribution of defective cable terminals are studied by using multi-physical field simulation method to realize the degree of axial development of faulty cable terminal. The electric field sensor was used to measure the surface field intensity distribution of cable terminals with different degrees of interface defects, and the electric field intensity distribution law of cable terminals with different degrees of defects is obtained. The distribution of the interquartile range and variance of the electric field intensity along the cable terminal is analyzed. The results show that the greater the interface defect, the greater the interquartile range and variance of the electric field intensity along the cable terminal. Therefore, the development degree of interface defects can be judged by testing the surface electric field intensity of cable terminal.

Keywords Cable terminal · Fault detection · Simulation · Internal defects · Electric field · Interquartile range · Variance

1 Introduction

High-voltage cable and its terminal of the high-speed electric multiple units (EMU) are the key equipment for train's power supply. It is mainly used to connect the high-voltage equipment of EMU and power transmission. Its safety is crucial to ensure

Y. Tang · Y. Xu · G. Gao · K. Liu (✉) · K. Chen · G. Wu
School of Electrical Engineering, Southwest Jiaotong University, Chengdu 611756, China
e-mail: 1129757680@qq.com

© Beijing Paike Culture Commu. Co., Ltd. 2024

X. Dong and L. Cai (eds.), *The Proceedings of 2023 4th International Symposium on Insulation and Discharge Computation for Power Equipment (IDCOMPU2023)*, Lecture Notes in Electrical Engineering 1102, https://doi.org/10.1007/978-981-99-7405-4_5

the safe and stable operation of EMU [1, 2]. The research data shows that the cable terminal is the weak link of the cable assembly [3, 4], and its failure rate over 70% [5]. Therefore, effectively and accurately grasping the insulation state of cable terminal is an important means to ensure the safe and reliable operation of EMU cable terminal.

Partial discharge detection is a commonly used electrical detection method. Partial discharge is often accompanied by sound, light, electromagnetic heat and other phenomena [6]. According to different characteristic signals, partial discharge detection methods are divided into pulse current method [7, 8], high frequency pulse current method [9, 10], ultra-high frequency method [11, 12]. However, partial discharge signal detection is susceptible to sensor sensitivity, field noise, external electromagnetic interference, signal attenuation and other factors. And how to extract and separate the information that can characterize the cable insulation state from the complex working condition environment is a problem faced by the current partial discharge insulation state detection. Therefore, it is very important to put forward new detection methods to improve the reliability of cable terminal operation, reduce the failure rate of EMU and ensure the safe operation of EMU.

In this paper, the multi-physical field simulation method was used to study the axial electric field distribution characteristics of the defective cable terminal, and the axial distribution location of the fault cable terminal was. realized. The electric field sensor is used to measure the surface field intensity distribution of cable terminals with different degrees of interface defects, and the electric field intensity distribution law of cable terminals with different degrees of defects is obtained. It provides the possibility for online diagnosis of cable terminal in the future.

2 Case Analysis

High-voltage cable terminal failure accident occurred frequently in a certain type of EMU in China. The faulty cable is shown in Fig. 1. The faulty cable terminal was disassembled and dissected on site. Through dissection, it was found that there were obvious traces of power generation between main insulation of the cable terminal and long strain control tube, as shown in the red dashed box in Fig. 1.

The cracking of the insulating sheath is the cause of the internal surface breakdown of the shed, and the air gap defect between the layers inside the shed is the main reason for the breakdown of the inner surface. When the air gap fault at the cable terminal interface, it will cause partial discharge inside the cable terminal. During the long-term operation of the EMU, the insulation degradation will be accelerated of the cable terminal, and eventually insulation failure, which will affect the safety of the EMU. safe and stable operation.

Fig. 1 The faulty cable terminal of high-speed train

3 Simulation Study

The finite element method is used to simulate the cable termination, which is mainly based on Maxwell's system of equations to construct the model and choose the static electric field to solve, Maxwell's system of equations is calculated as follows [13].

$$\nabla \times H = J + \frac{\partial D}{\partial t} \tag{1}$$

$$\nabla \times E = 0 \tag{2}$$

$$\nabla \cdot B = 0 \tag{3}$$

$$\nabla \cdot D = \rho \tag{4}$$

where H is the magnetic field strength, E is the electric field strength, J is the full current density, D is the electric induction strength; B is the magnetic induction strength. At the same time each linear material medium of the cable terminal needs to satisfy the following intrinsic relationship [13].

$$D = \varepsilon E \tag{5}$$

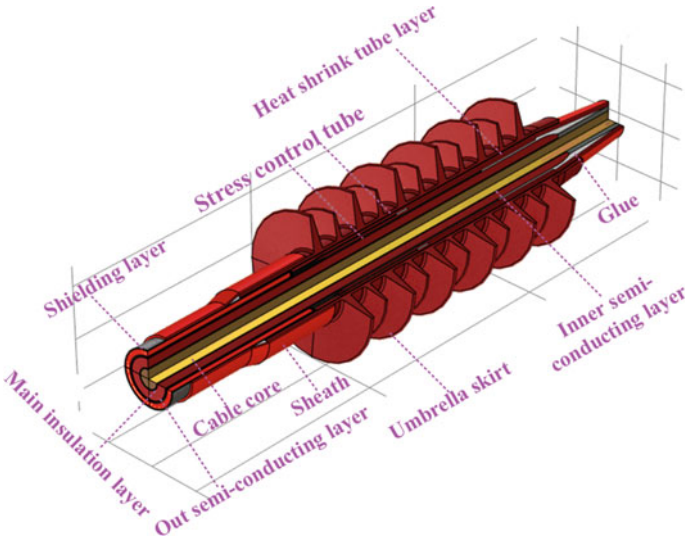

Fig. 2 Three-dimensional structure of cable terminal

$$J = (\sigma + j\omega\varepsilon)E \tag{5}$$

where ε is the dielectric constant, σ is the electrical conductivity, B is the magnetic induction, ω is the magnetic permeability, and is the angular frequency.

Based on the actual model structure of the on-board high-voltage cable terminal, the cable terminal model diagram was constructed using COMSOL simulation software, and the model was built according to the actual terminal scale of 1:1, and the cable terminal model was constructed as shown in Fig. 2.

4 Simulation Results

In this paper, the length of the first layer of the high voltage cable terminal is defined as l, and its length is 260 mm. The air gap length is used to describe the degree of defects. Defects are constructed in the main insulation and the first layer of stress tube. The defect lengths l' are 0.55 and 100%l, respectively. In order to simulate the actual discharge effect inside the cable terminal, carbon marks were used to replace air gap defects. Figure 3 is the schematic diagram of the cable terminal defect model.

Figure 4 and Table 1 statistics of the electric field intensity results inside the defective cable terminal. When there is no defect inside the cable terminal, the maximum electric field intensity inside it is mainly at the location where the three phases of the main insulation, the outer semi-conducting layer and the long stress control tube are combined, such as at the location of the red circle in Fig. 4. As the voltage level

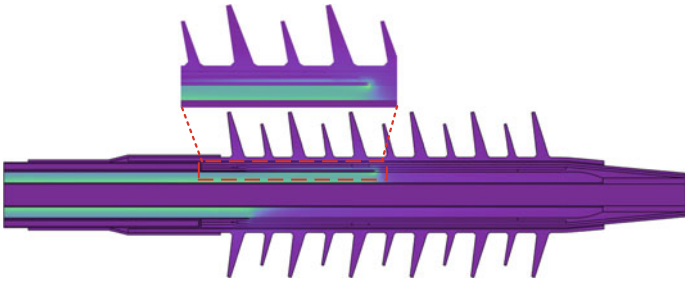

Fig. 3 Schematic diagram of carbon mark defect at cable terminal interface

increases, the intensity of its internal distortion electric field gradually increases. When there is a defect between the main insulation and the long control tube inside the cable terminal, the maximum distortion position inside the cable terminal appears at the defective end position. With the increase of defects, the electric field strength of internal distortion of the cable gradually increases at the same voltage level.

In the cable terminal large umbrella skirt surface 2 mm set air domain, along the main insulation and the first layer should control the tube interface between the carbon trace vertical direction at the electric field strength marked as E_0, cable terminal electric field strength starting test electric field position and cut-off position as shown in Fig. 5.

In order to clarify the relationship between the degree of defect development at the cable termination interface and the electric field tested along the surface, the electric field intensity values tested at different locations were processed in this study, and

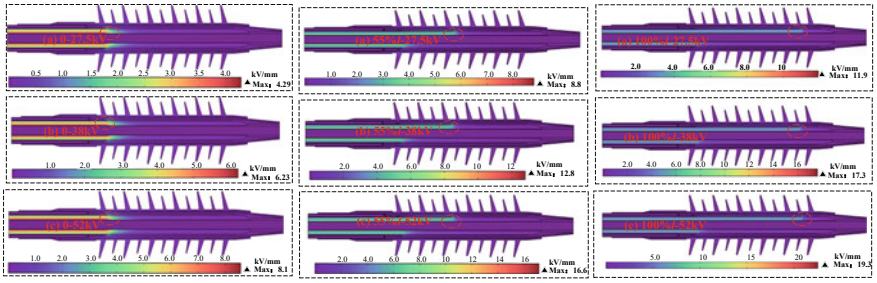

Fig. 4 Electric field strength inside the cable terminal

Table 1 Electric field intensity statistics inside the cable terminal

	10 kV	20 kV
0 (kV/mm)	1.65	3.12
55%*l* (kV/mm)	3.34	6.4
100%*l* (kV/mm)	4.33	8.67

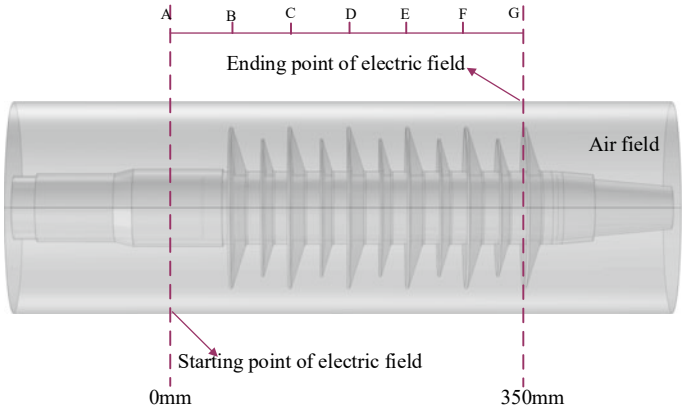

Fig. 5 Cable terminal simulation electric field test location

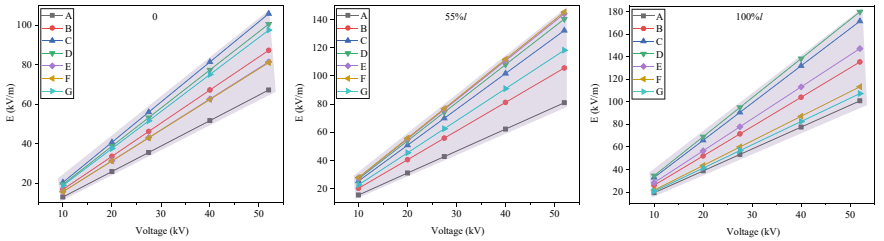

Fig. 6 Statistics of electric field strength of defective cable terminals under different voltage levels

the degree of defect development at the cable termination interface was expressed using the parameters of *Interquartile Range* (IR) and *Variance.*

The Interquartile Range [14] is the difference between the 3rd quartile and the 1st quartile, also known as the internal distance or quartile spacing, and is denoted by Q_r. The IR is calculated as $Q_r = Q_3 - Q_1$. The quartiles reflect the degree of dispersion of the middle 50% of the data. The smaller the value, the more centralized the data in the middle. The smaller the value, the more concentrated the data in the middle, the larger the value, the more dispersed the data in the middle. Q_1 and Q_3 are calculated by the formula:

$$\mathrm{Q}_1 = L + \frac{\frac{n+1}{4} - F}{f} i \tag{7}$$

$$\mathrm{Q}_3 = L + \frac{\frac{3(n+1)}{4} - F}{f} i \tag{8}$$

where, L is the lower bound of the group in which the *IR*, F is the cumulative frequency, f is the frequency, and i is the width of the group.

In statistics, variance is used to calculate the difference between each variable and the population mean. Variance describes the degree of dispersion of the value of a random variable to its mathematical expectation. The calculation formula is as follows:

$$S^2 = \frac{\sum (X - \overline{X})^2}{n - 1} \tag{9}$$

where S^2 represents the sample variance, X is the variable, $\overline{X}$ is the sample mean, and n is the number of samples.

The statistical results of *IR* of electric field strength at the cable terminal were shown in Fig. 7.

$$y = ax + b \tag{10}$$

where y is the *IR* of field intensity, x is the voltage level, a is the slope, and b is the intercept. As can be seen from Fig. 7, with the increase of interface defects, the IR of electric field intensity also increases, resulting in greater dispersion of electric field intensity at different locations. The larger the defect, the greater the IR slope of the electric field intensity. When the interface defect increased from 20 to 100%l, the IR slope of electric field intensity increased from 0.34 to 1.01.

Figure 8 shows the variance of electric field intensity. The variance of electric field intensity measured at different voltages meets the following fitting formula:

$$y = y_0 + A_1 e^{x/t_1} \tag{11}$$

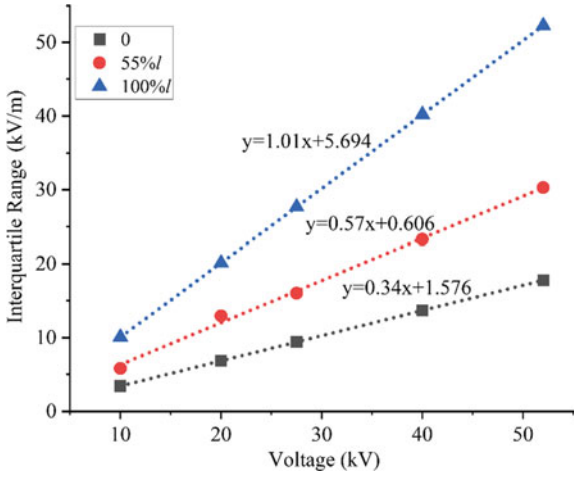

Fig. 7 Interquartile range of simulation

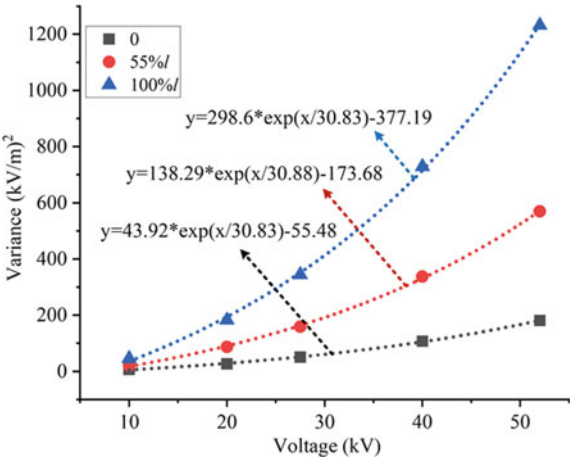

Fig. 8 Electric field strength variance statistics of simulation

where y_0 refers to the offset, A_1 refers to the preexponential, and t_1 refers to the relaxation time.

It can be seen from the statistical results that as the interface defects gradually increase, the variance of the electric field strength of the cable terminal also gradually increases. The larger the defect, the larger the pre-exponential factor of the electric field intensity variance at different positions, and the absolute value of the electric field intensity variance offset gradually increases. When the interface defect of the cable terminal is 100%*l*, the pre-exponential factor and the absolute value of the offset of the fitting parameters of the electric field intensity variance are 298.6 and 377.19, respectively. Compared with the defect-free cable terminal, the absolute value of the pre-exponential factor and the offset of the electric field intensity variance increased by about 85.3% and 85.29%, respectively. However, the relaxation time changes irregularly with the increase of interface defects.

5 Experiments and Test Results

In this paper, different lengths of air gap defective cable terminal are prepared, and the length of the first layer of stress control tube inside the high voltage cable terminal is defined as *l*. The air gap length was used to describe the degree of defects, and the defect lengths l' are 0, 55, 100%*l*. Use a carbon pen to draw a line from point A according to the predetermined defect length (hereinafter referred to as "carbon mark"). Make sure the carbon marks are clear and the width is not less than 1mm. A wire with a diameter of 2 mm is pre-buried next to the carbon trace. The prefabricated defective cable terminal is shown in Fig. 9.

The schematic diagram of the sensor test arrangement is shown in Fig. 10.

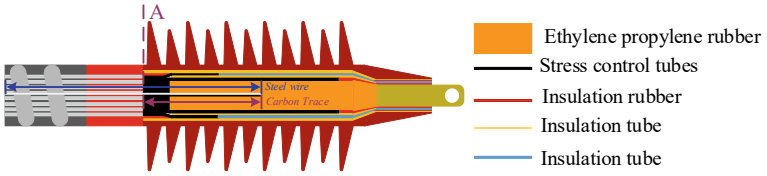

Fig. 9 Prefabricated defect cable terminal schematic diagram

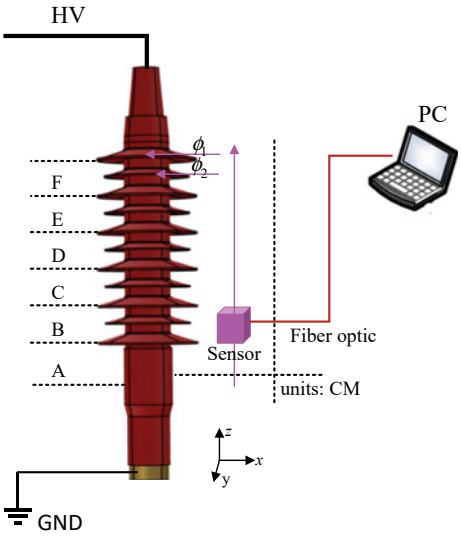

Fig. 10 Schematic diagram of electric field sensor arrangement along the cable terminal surface

The result of testing the cable termination strength quadrature difference value by test is shown in Fig. 11. The linear relationship between the test electric field strength quartile difference value and voltage is good. The larger the defect is, the larger the slope of the test field strength quartile difference is. When the interface defect increases from 20 to 100%l, the slope of the electric field strength quadrature difference increases from 0.076 to 0.679, which is consistent with the simulation results.

Figure 12 shows the statistics of the electric field strength variance of the cable termination test, and the trend is consistent with the simulation results. From the statistical results, it can be seen that with the gradual increase of interface defects, the variance of electric field strength at cable terminals also gradually increases. The variance fitting parameters of the cable termination specimens with 0, 55 and 100%l are 2.76, 62.86 and 109.42; the absolute values of the variance fitting parameters offset were 3.33, 85.51 and 126.71, respectively. the larger the defect, the larger the variance fitting factors of the electric field strength at different locations, and the absolute values of the electric field strength variance offset also increased gradually.

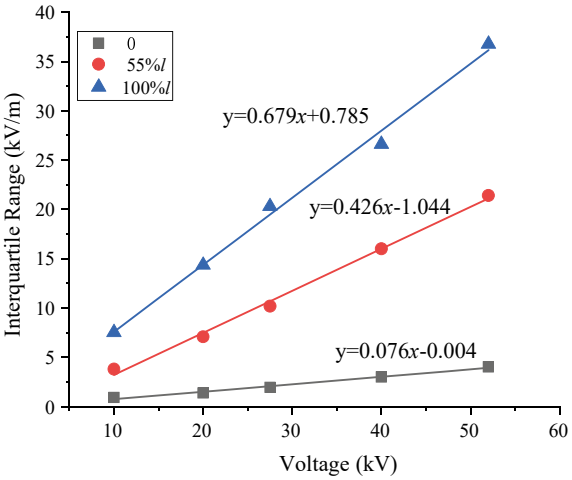

Fig. 11 The interquartile range of experiment

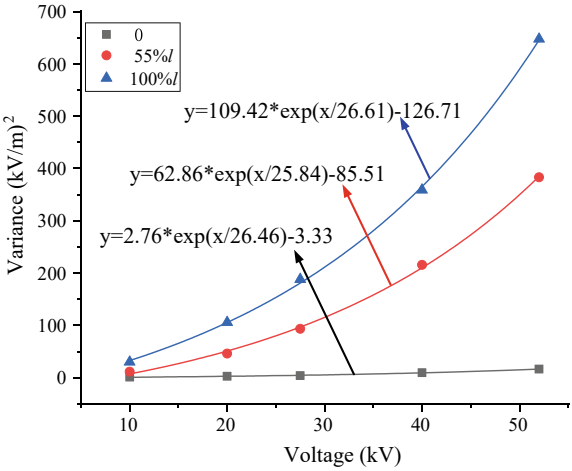

Fig. 12 The variance of experiment

The simulation and experimental test results are consistent. By testing the electric field strength along the umbrella skirt of the cable terminal, the development degree of internal defects in the cable terminal can be effectively reflected. Compared with traditional cable terminal fault detection methods, this method is simple to test and has strong anti-interference ability.

6 Conclusion

The following conclusions are obtained:

(1) With the increase of voltage level, the electric field intensity along the surface of the cable terminal also gradually increases, and the linear relationship between electric field intensity and voltage level is good. As the interface air gap defects are larger, the electric field strength dispersion of cable terminals at different axial positions is obviously inconsistent. The larger the interface air gap defects, the greater the interquartile range and variance of the electric field strength at different locations, the greater the electric field strength dispersion.
(2) By arranging multiple sensors along the surface of the cable terminal, the internal fault of the cable terminal can be detected quickly and effectively, effectively improving the sensitivity of cable terminal insulation fault detection; therefore, the reasonable arrangement of electric field sensors can be used for the detection of internal defects of the cable terminal, determining the degree of development of internal defects of the cable terminal and assisting in deciding whether the cable terminal needs to be replaced.

Acknowledgments This work is supported by National Natural Science Foundation of China (U1966602) and Excellent Young Scientists Fund of China (51922090).

References

1. Bai L, Zhou L, Li L, Chen Y, Guo L (2019) Partial discharge of cable termination on EMU of China high-speed railway below zero degrees centigrade. IET Sci Meas Technol 13(6):912–921
2. Zhou L, Zhu S, Bai L, Liu Y, Zhu L, Guo L (2019) Influence of stress tubes interface on partial discharge of vehicle cable terminal at low temperatures. High Voltage Eng 45(4):1266–1273
3. Mazzanti G, Marzinotto M (2017) Advanced electro-thermal life and reliability model for high voltage cable systems including accessories. IEEE Electr Insul Mag 3(33):17–25
4. Lai Q, Chen J, Hu L, Cao J, Xie Y, Guo D, Liu G, Wang P, Zhu N (2020) Investigation of tail pipe breakdown incident for 110 kV cable termination and proposal of fault prevention. Eng Fail Anal 108:104353
5. Du B, Han T (2014) Tree characteristics in silicone rubber/SiO_2 nanocomposites under low temperature. IEEE Trans Diel Electron Ind 21(2):503–510
6. Nie YJ, Zhao XP, Li ST (2020) Research progress in condition monitoring and insulation diagnosis of XLPE cable. High Voltage Eng 464:1361–1371
7. Chou CJ, Chen CH (2018) Measurement and analysis of partial discharge of high and medium voltage power equipment. In: 2018 7th International symposium on next generation electronics (ISNE), Taipei, Taiwan
8. Bai LL, Zhou LJ, Cao WD, Che XY, Xing LM, Li LN (2020) Characteristics of partial discharge in air gap defects in EPR cable termination under −40 °C condition. High Voltage Eng 4610:3605–3614
9. Álvarez F, Garnacho F, Ortego J, Sánchez-Urán M (2015) Application of HFCT and UHF sensors in on-line partial discharge measurements for insulation diagnosis of high voltage equipment. Sensors (Basel, Switzerland) 15:7360–7387

10. Yii CC, Rohani MNKH, Isa M, Hassan SIS (2017) Multi-end PD location algorithm using segmented correlation and trimmed mean data filtering techniques for mv underground cable. IEEE Trans Dielectr Electr Insul 24:92–98
11. Ma S, Chen M, Wu J, Wang Y, Jia B, Jiang Y (2019) High-voltage circuit breaker fault diagnosis using a hybrid feature transformation approach based on random forest and stacked autoencoder. IEEE Trans Ind Electron 66:9777–9788
12. Dey D, Chatterjee B, Dalai S (2018) A deep learning framework using convolution neural network for classification of impulse fault patterns in transformers with increased accuracy. IEEE Trans Dielectr Electr Insul 24(6):3894–3897
13. Hayt AJ Jr, William H, Buck JAS (2018) Buck engineering electromagnetics. Xi'an Jiaotong University Press, Xi'an
14. Zhao TH, Zhang Y, Wang JX (2021) Load outlier identification method based on spatial density clustering and abnormal data domain. Autom Electric Power Syst 45